SIMULATION STUDIES OF THE X-RAY FREE-ELECTRON LASER OSCILLATOR*

R.R. Lindberg †, Y. Shyd'ko, K.-J. Kim, ANL Advanced Photon Source, Argonne, IL 60439, USA
W. M. Fawley, LBNL Center for Beam Physics, Berkeley, CA 94720, USA

Abstract

Simulations of the x-ray free-electron laser (FEL) oscillator are presented that include transverse effects and realistic Bragg crystal properties with the two-dimensional code GINGER. In the present cases considered the radiation divergence is much narrower than the crystal acceptance, and the numerical algorithm can be simplified by ignoring the finite angular bandwidth of the crystal. In this regime GINGER shows that the saturated x-ray pulses have $\sim 10^9$ photons and are nearly Fourier-limited with peak powers in excess of 1 MW. We also include preliminary results for a four-mirror cavity that can be tuned in wavelength over a few percent, with future plans to incorporate the full transverse response of the Bragg crystals into GINGER to more accurately model this tunable source.

INTRODUCTION

First proposed by Colella and Luccio 25 years ago [1], there has been renewed interest in an x-ray free-electron laser (FEL) oscillator with the recent set of concrete, realizable parameters put forth by Kim, Shvyd'ko and Reiche [2]. As shown in Ref. [2], the x-ray FEL oscillator can produce fully coherent x-ray pulses with MWs of power by combining an ultra-low emittance, low charge electron beam and a resonator cavity formed using high-reflectivity, narrow-bandwidth Bragg crystals. This paper presents some recent simulation results including the full frequency-dependent reflectivity of the Bragg crystals and the transverse effects of beam divergence and radiation diffraction using the two-dimensional axisymmetric code GINGER [3]. First, we discuss the two-crystal cavity near-backscatter, including a summary of the relevant new physics and simulation results from a number of possible designs that show spectrally pure pulses of $\sim 10^9$ photons and third harmonic generation with $\sim 10^5$ photons at 36 keV. Next, we present results relevant to a tunable, four-mirror cavity for which similar pulse characteristics are observed. Finally, we discuss future extensions and conclude.

TWO-CRYSTAL CAVITY

The two-crystal x-ray FEL oscillator cavity is a simple extension of the stable two-mirror resonator familiar from laser optics (see, e.g., [4]). In this geometry, x-rays are contained by two Bragg crystals operating in near-backscatter geometry, while focusing is provided by grazing incidence mirrors as shown in Fig. 1(a). In the next subsection we briefly highlight the most relevant issues introduced by inclusion of transverse physics (i.e., beam divergence, radiation diffraction, and x-ray focusing) and the complex reflectivity of the Bragg mirrors. We then present a set of simulation results for the two-mirror cavity geometry over a range of wavelengths using a variety of Bragg crystal, electron beam, and undulator parameters. We find that third harmonic emission may provide an interesting source of radiation beyond 20 keV energy.

Simulations Including Transverse Physics and Bragg Crystal Properties

Typical electron beam parameters for the x-ray FEL oscillator include a bunch length $\sigma_e \sim 1$ ps, peak current $I_{\rm peak} \sim 10$ A, normalized emittance $\epsilon_{x,n} \sim 10^{-7}$ mm $\cdot$ mrad, and normalized energy spread $\sigma_\eta \sim 0.02\%$; specific examples are listed in Table 1. These parameters are chosen so that a low-charge electron bunch of energy $E_{\rm beam} = 7$ GeV will give rise to a single pass FEL gain $g_{\rm linear} \gtrsim 0.3$ over $N_u \sim 3000$ periods of undulator. In the low-gain regime, the FEL gain is typically maximized when the transverse spreading of the radiation matches that of the electron beam, $z_R \approx z_\beta$, where z_R is the x-ray Rayleigh range while the (vacuum) beam focusing parameter z_β is related to the emittance ϵ_x and transverse size σ_x at position z via

$$\sigma_x(z) = z_\beta \epsilon_x \left[1 + (z - z_0)^2/z_\beta^2\right]. \qquad (1)$$

The gain is maximized when the electron beam waist is located at the middle of undulator length L_u, $z_0 = L_u/2 = N_u\lambda_u/2$, and when the focusing parameter $z_\beta \approx L_u/2\pi$ [5]. With $z_\beta \approx z_R$, maximizing the gain for a fixed cavity length in turn sets the grazing incidence mirror focal length. Presently, GINGER approximates mirror focusing by an ideal thin lens.

The reflective properties of near-perfect Bragg crystal reflectors are described by the theory of dynamical diffraction (see, e.g., [6]). The basic results of this theory show that Bragg crystals coherently reflect radiation in a narrow spectral band near that defined by Bragg's Law: $E = E_H/\cos\theta$, where E is the photon energy, θ is the incidence angle from normal, and E_H is the Bragg energy, which is related to the crystalline planar spacing d through the speed of light c and Planck's constant h by $E_H \equiv hc/2d$. The weak angular dependence for $\theta \ll 1$ in near-backscatter implies that the finite angular acceptance of the crystal can

* Work supported by U.S. Dept. of Energy, Office of Science, Office of Basic Energy Sciences, under Contract No. DE-AC02-06CH11357

† lindberg@aps.anl.gov

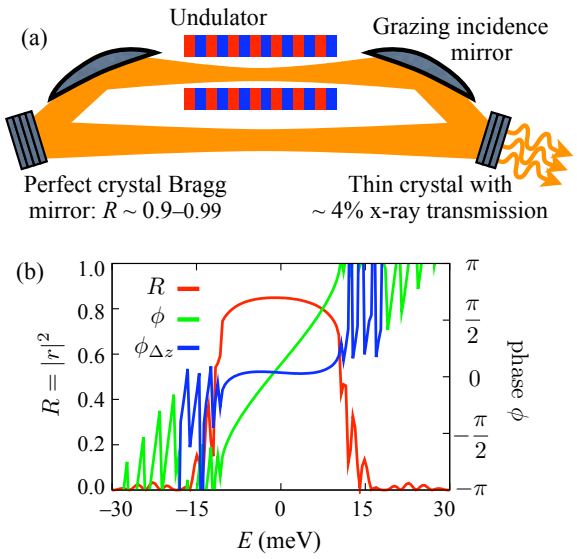

Figure 1: Panel (a) shows a schematic of the two-mirror x-ray FEL cavity, including the stable x-ray mode in the undulator as defined by the grazing incidence mirrors and the two Bragg crystals. The crystal on the right is thin so as to transmit $\sim$4% of the cavity radiation. Panel (b) shows the total reflectivity R for two C(4 4 4) crystals (one thick and one thin) and the complex phase of the amplitude reflectivity $r = |r|e^{i\phi}$, with $|r|^2 = R$. Note how the phase ϕ (green line) is approximately linear within the Darwin width, which can be nearly cancelled by decreasing the cavity length to form the blue line $\phi_{\Delta z}$. For this C(4 4 4) crystal, the optimal cavity length reduction is 32 μm.

be ignored. Unfortunately, it also severely limits the degree to which one may tune the photon energy.

Previous work on the x-ray FEL oscillator [2, 7] focused on the small spectral acceptance of the Bragg crystals, finding that the inverse width of the electron beam must be smaller than the frequency bandwidth of the crystals in order not to adversely affect gain. As shown by the green line in Fig. 1(b), the complex reflectivity also varies in phase ϕ within the region of high reflectivity (the Darwin width). The nearly linear variation in phase with energy delays the x-ray pulse in time. Physically, this delay comes about because the Bragg crystal reflects x-rays via the coherent superposition from many crystal planes, so that the radiation effectively penetrates some distance into the crystal. Thus, we can largely cancel the phase shift near peak reflectivity by decreasing the cavity length. To demonstrate this, we plot the total complex phase $\phi_{\Delta z}$ including both the crystal reflectivity and a cavity length detuning Δz by the blue line. In this case, the phase is nearly constant within the Darwin width, implying that the radiation suffers minimal delay or distortion from pass to pass. For the diamond crystal C(4 4 4) near 1 Å shown in Fig. 1 the cavity length was decreased by 32 μm.

Within GINGER, we include the crystal complex reflectivity as a function of wavelength such as that represented in Fig. 1(b) with a separate input data file. After each pass the radiation is Fourier transformed, multiplied by the complex crystal reflectivity, and then inverse Fourier transformed back to the time domain for the next pass.

Radiation Characteristics and FEL Performance

We list the parameters and radiation characteristics for a range of radiation wavelengths in Table 1. As mentioned previously the parameters were tailored so that a low-charge ($\lesssim$50 pC) beam can provide sufficient linear FEL gain to overcome the losses, which include the photoabsorptive losses in the crystals, the $\sim$4% radiation that is coupled out of the cavity through the thin Bragg crystal, and an assumed 5% loss for each of the two focusing mirrors. As indicated by Table 1, crystal photo-absorption is smallest for diamond (typically $R \sim 99\%$ for a thick diamond crystal), while the reflectivity in sapphire is $\sim$97% and $\sim 90\%$ for silicon crystals. The high peak reflectivity, coupled with its low coefficient of thermal expansion and high coefficient of thermal conductivity, make diamond the ideal Bragg crystal for the x-ray FEL oscillator.

The bottom portion of Table 1 lists the radiation properties, starting with the saturated power $P_{\rm sat}$ in the cavity, and continuing with the characteristics of the x-ray pulses following transmittion through the thin mirror. The peak power of the out-coupled radiation is predicted to be between 0.5 and 2.5 MW; this relatively narrow range of output powers arises because we have chosen the parameters to have similar linear gains which saturate at comparable radiation amplitudes. The output pulses contain $\sim 10^9$ photons that are nearly Fourier limited; because of the extremely narrow meV bandwidth, these x-ray pulses are predicted to have a peak spectral brightness of $\sim 10^{32}$ photons/[sec $*$ (mm-mrad)^2 $*$ (0.1% BW)].

Harmonic Emission

Table 1 indicates that at saturation the FEL oscillator typically produces a megawatt of nearly transform-limited x-ray power at the fundamental wavelength. At saturation the electron bunching is quite strong and has significant Fourier content at higher harmonics. In a linearly-polarized undulator, these components will in turn generate coherent radiation at odd harmonics of the fundamental photon energy. Preliminary results indicate that the power in the third harmonic can be $\sim 10^{-4}$ to 10^{-3} of that in the out-coupled fundamental (i.e., $\sim 10^{-6}$ to 10^{-5} of the intercavity power), leading to 10^2 to 10^3 W of coherent energy between 30 and 60 keV.

Naïve scaling of previous experiments at IR wavelengths (e.g., [8, 9]) would yield powers in the third harmonic that are one to three orders of magnitude larger than what we have obtained in GINGER for x-rays. There are two main differences that account for this discrepancy. The first is that due to the longer penetration length at shorter wavelengths, the thin Bragg mirror is nearly transparent to the

Table 1: FEL parameters and radiation characteristics obtained from GINGER for the two-cavity x-ray FEL oscillator. The electron beam normalized emittance, energy spread, and width are fixed at $\epsilon_{x,n} = 0.2$ mm $\cdot$ mrad, $\sigma_\eta = 0.02\%$, and $\sigma_e = 1$ ps, respectively, while the remaining parameters are adjusted to yield positive net gain: $g_{\text{linear}}(1 - R_{\text{total}}) > 1$. The power P_{sat} refers to inter-cavity power at saturation, while the spectral properties, photons/pulse, and P_{peak} listed at the bottom refer to steady-state quantities of the radiation after being transmitting through the thin mirror.

Parameter	4.92 keV	5.59 keV	12.04 keV	14.32 keV	19.94 keV
λ_u (cm)	2.24	1.96	1.76	1.66	1.50
N_u	1000	1500	3000	3000	3000
FEL K	2.50	1.53	1.51	1.32	1.05
E_{beam} (GeV)	7.0	5.0	7.0	7.0	7.0
I_{peak} (A)	10.0	20.0	10.0	20.0	20.0
Z_β (m)	4.5	6.0	10.0	10.0	10.0
g_{linear}	0.32	0.60	0.36	0.55	0.32
R_{total}	0.84	0.66	0.85	0.80	0.85
Bragg crystal	C(2 2 0)	Si(2 2 4)	C(4 4 4)	AlO(0 0 0 30)	C(5 5 9)
Crystal $\Delta\lambda/\lambda$	10^{-5}	3×10^{-6}	10^{-6}	5×10^{-7}	10^{-7}
P_{sat} (MW)	99.0	22.7	25.8	25.2	12.9
spectral width (meV)	2.89	2.16	1.29	2.54	0.80
$\Delta t \Delta\omega$	2.25	1.38	1.01	2.90	1.14
photons/pulse	4.6×10^9	6.0×10^8	1.1×10^9	6.2×10^8	3.6×10^8
P_{peak} (MW)	2.5	1.5	1.66	0.78	0.57

third harmonic. Thus, the x-ray output at the third harmonic is only that which is generated over a single pass. The second explanation for the lower power is the comparatively large (scaled) energy spread of the x-ray FEL oscillator. As discussed in [8, 10], there is significant reduction in harmonic output when the normalized energy spread σ_η becomes larger than $2\pi N_u^{-1}$. While most previous experiments operated near or below $2\pi N_u \sigma_\eta = 1$, in the x-ray FEL oscillator this quantity is approximately 4. The large σ_η leads to destructive interference whose effect is more pronounced as the harmonic number increases.

Although the harmonic power may be somewhat less than what one might expect, nevertheless it is still an interesting source of radiation beyond 20 keV. For example, using the parameters for the 12 keV source in Table 1, we find that harmonic generation provides 2×10^4 coherent photons at 36 keV. Increasing the current to 20 A increases the energy at 12 keV by a factor of 3 while raising the energy at the third harmonic by nearly a factor of 30, producing 5×10^5 photons at 36 keV.

FOUR-MIRROR CAVITY

While the two-mirror cavity is simple in conception and design, this design requires near-backscatter reflections on the Bragg crystals for the grazing incidence mirrors to provide a low-loss, closed circuit. The backscatter requirement $\theta \ll 1$ and Braggs Law $E = E_H/cos\theta$ severely limits the operational tuning range for an x-ray FEL oscillator based on a two-mirror cavity. Changing to a four-mirror geometry can significantly increase this range, fortunately. The basic design is the "bow-tie" geometry shown in Fig. 2(a) which relaxes the two-mirror backscatter requirement. As shown in [11], by simultaneously adjusting the four path lengths and the incidence angles on the crystals, one can vary the resonant photon energy while keeping the radiation transit time constant.

We list the preliminary simulation results from such a four-mirror design operating at three different photon energies in Table 2. Note that these results are similar to those in the two-mirror Table 1, although to overcome the additional losses we increased the peak current to 20 A in all cases. Additionally, we include two separate results for the 9 and 14 keV cases, one for which the mirror and crystal reflectivities are near their optimal value, and the second in which we assumed a less-than-ideal scenario resulting in an additional $\sim 10\%$ loss. While the decreased reflectivity halves the output power, the x-ray pulses are coherent and nearly Fourier limited. The fractional energy range over which the FEL gain overcomes losses is nearly 5%. Finally, the results in Table 2 were obtained by averaging the four-mirror reflectivity over the angle θ assuming a 0.25 μrad radiation angular divergence as expected from the cavity and focusing design. We show an example of this in Fig. 2(b); since the angular acceptance of the crystal is much greater than the divergence of the radiation we expect such an approximation to be valid, however future work must include the full transverse response of the crystals.

FUTURE DIRECTIONS

We have shown that a FEL oscillator using narrow bandwidth Bragg crystals can in principle provide a source of MW x-ray pulses that are fully transversely and longitudinally coherent. Nevertheless, there remain some important issues that yet need to be addressed. One main avenue that

Table 2: FEL parameters and radiation characteristics obtained from GINGER simulations for the four-cavity x-ray FEL oscillator. Electron beam parameters are the same as Table 1, except $I_{\rm peak} = 20$ A. For all simulations, $z_\beta = 10$ m and $N_u = 3000$. The radiation characteristics listed at the bottom are measured inside the cavity, and for the two lower energies are listed for the "idealized" reflectivities on the left and the more conservative ones on the right, as described in the text.

Parameter	9.131 keV		14.4125 keV		20.514 keV
λ_u (cm)	1.76		1.66		1.50
N_u	3000		3000		3000
FEL K	1.52		1.32		1.05
$\epsilon_{x,n}$ (mm·mrad)	0.2		0.2		0.1
$g_{\rm linear}$	0.86		0.58		0.56
Bragg crystal	C(3 3 3)		C(3 3 7)		C(3 3 11)
Tuning range	6.2%		6.0%		3.5%
	$R_{\rm tot} = 0.81$	$R_{\rm tot} = 0.72$	$R_{\rm tot} = 0.83$	$R_{\rm tot} = 0.73$	$R_{\rm tot} = 0.83$
$P_{\rm sat}$ (MW)	98	45	51	22.5	40
spectral width (meV)	1.01	1.10	0.548	0.434	0.534
$\Delta t \Delta\omega$	1.05	0.93	1.39	1.13	0.71
Cavity photons/pulse	115×10^9	49×10^9	29×10^9	10×10^9	23×10^9

we plan to explore is a more complete description of the radiation propagation outside the undulator. Specifically, we would like to include a more general series of vacuum sections between which we can more accurately model the grazing incidence mirror properties and aberrations and account for the finite angular acceptance of the Bragg mirrors. This work would also open a path for addressing mirror and crystal tolerances concerning positioning, stability, and roughness. The other extension will involve including particle data obtained from simulations of the high-brightness electron cathode, injector, and accelerator. In this way, the interplay between the electron beam, the x-ray optics, and the radiation generation can be more completely explored.

REFERENCES

[1] R. Colella and A. Luccio, Optics Comm. 50 (1984) 41.

[2] K.-J. Kim, Y. Shvyd'ko and S. Reiche, Phys. Rev. Lett. 100 (2008) 244802.

[3] W. M. Fawley, tech. rep. LBNL-49625 (2002).

[4] A. E. Siegman, *Lasers*, University Science Books, NY, NY (1986).

[5] K.-J. Kim, Nucl. Instrum. Methods A 318 (1992) 489.

[6] Y. Shvyd'ko, *X-Ray Optics - High Energy-Resolution Applications*, Springer, NY, NY (2004).

[7] R. R. Lindberg and K.-J. Kim, Phys. Rev. ST-AB 12 (2009) 070702.

[8] D. J. Bamford and D. A. G. Deacon, Nucl. Instrum. Methods A 285 (1989) 23.

[9] R. Hajima, R. Nagai, N. Nishimori, N. Kikuzawa, and E. J. Minehara, Nucl. Instrum. Methods A 475 (2001) 43.

[10] H. P. Freund, R. C. Davidson, and D. A. Kirkpatrick, Nucl. Instrum. Methods A 318 (1992) 477.

[11] K.-J. Kim and Y. Shvyd'ko, Phys. Rev. ST-AB 12 (2009) 030703.

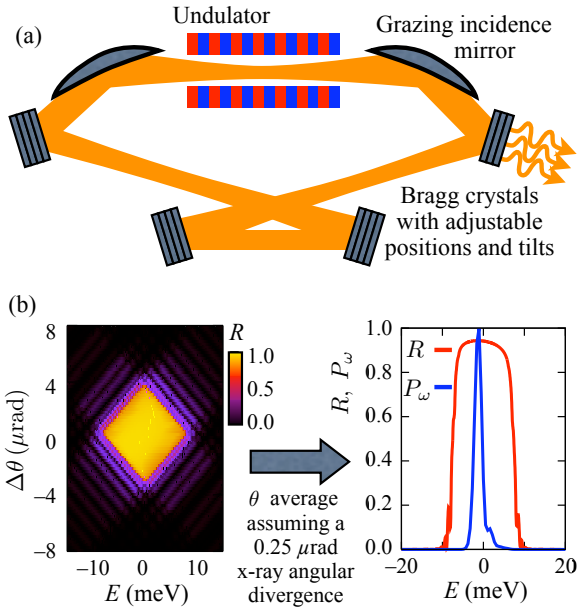

Figure 2: Panel (a) shows a schematic of the four-mirror x-ray FEL cavity, for which the mirror angle θ can be adjusted to vary the photon energy through $E = E_H/\cos\theta$, while simulataneously preserving the round-trip time-of-flight. The left plot of panel (b) shows the four-mirror reflectivity of the C(3 3 7) reflection at $\theta = 15^\circ$ as a function of the frequency and angular deviation. Note that the angular acceptance is much less than the expected x-ray divergence $\sim 0.25\mu$rad, so that the average over θ leading to the right-hand plot of the reflectivity (red line) should be approximately valid. GINGER 12-keV simulation results (blue line) illustrate the narrow meV-scale bandwidth of the FEL output at saturation.